



Research article



Statistical influence of NH_4OH , number of layers and droplet volume in the development of ultra-hydrophobic coatings based on SiO_2 nanoparticles

Influencia estadística del NH_4OH , número de capas y volumen de gota en el desarrollo de recubrimientos ultra-hidrofóbicos basados en nanopartículas de SiO_2

José Felix Magdaleon Loredo , Delfino Cornejo Monroy 

Instituto de Ingeniería y Tecnología, Universidad Autónoma de Ciudad Juárez. Av. Del Charro 450 Norte, Col. Partido Romero 32310, Ciudad Juárez, Chihuahua, México

Corresponding author: Jose Felix Magdaleon Loredo, Instituto de Ingeniería y Tecnología, Universidad Autónoma de Ciudad Juárez. Av. Del Charro 450 Norte, Col. Partido Romero 32310, Ciudad Juárez, Chihuahua, México. E-mail: al198636@alumnos.uacj.mx. ORCID: 0000-0002-2043-2842

Recibido: 18 de Septiembre del 2021 **Aceptado:** 22 de Diciembre del 2021 **Publicado:** 13 de Enero del 2022

Abstract. – Ultra-hydrophobic coatings are of interest in automotive, aeronautical and construction applications and in general in any area or surface where the use of highly water-repellent surfaces, with self-cleaning, anti-icing, and anti-corrosion properties is favorable. In recent years, various researchers have proposed different physical and chemical methods to obtain high-hydrophobic condition. In this article, the manufacture of a colloid based on SiO_2 nanoparticles is described to manufacture hydrophobic coatings with contact angles greater than 140° . With the help of a design of experiments and the manufacture of a colloid based on SiO_2 by the colloidal method, three factors were analyzed with their corresponding levels and their influence to maximize the contact angle. The fabricated colloid was sprayed and layered onto glass. In all the materials where the coating was applied, static contact angles (SCA) between 120° and 160° were obtained. Results by UV-Vis's spectroscopy indicate that the transparency is greater than 68% and that this depends directly on the layers applied by spraying and on the quality of the film formed. The FT-IR spectra support the formation of SiO_2 nanoparticles, the presence of -OH groups in the different stages of the colloid manufacturing process, and C-F bonds. The composition and morphology were analyzed by field emission scanning electron microscopy (FESEM). FESEM micrographs were analyzed for the ultra-hydrophobic solutions and showed agglomeration of nanoparticles. As work in the future, it is proposed to analyze the wear resistance of coatings, their durability, and sliding angle, improving their hydrophobic properties.

Keywords: Ultra-hydrophobic coatings; Design of experiments; SiO_2 nanoparticles; Sol-gel method; Transparency.

Resumen. – Los recubrimientos ultra-hidrofóbicos son de interés en aplicaciones de automoción, aeronáutica y construcción y en general en cualquier zona o superficie donde sea favorable el uso de superficies altamente hidrofugantes, con propiedades autolimpiantes, antihielo y anticorrosión. En los últimos años, varios investigadores han propuesto diferentes métodos físicos y químicos para obtener una condición altamente hidrofóbica. En este artículo se describe la fabricación de un coloide a base de nanopartículas de SiO_2 para fabricar recubrimientos hidrofóbicos con ángulos de contacto superiores a 140° . Con la ayuda de un diseño de experimentos y la fabricación de un coloide a base de SiO_2 por el método coloidal, se analizaron tres factores con sus correspondientes niveles y su influencia para maximizar el ángulo de contacto. El coloide fabricado se pulverizó y se colocó en capas sobre el vidrio. En todos los materiales donde se aplicó el recubrimiento se obtuvieron ángulos de contacto estático (SCA) entre 120° y 160° . Los resultados por espectroscopía UV-Vis indican que la transparencia es superior al 68% y que esto depende directamente de las capas aplicadas por proyección y de la calidad de la película formada. Los espectros FT-IR respaldan la formación de nanopartículas de SiO_2 , la presencia de grupos -OH en las diferentes etapas del proceso de fabricación de coloides y enlaces C-F. La composición y morfología se analizaron mediante microscopía electrónica de barrido por emisión de campo (FESEM). Las micrografías FESEM se analizaron en busca de soluciones ultra hidrofóbicas y mostraron aglomeración de nanopartículas. Como trabajo a futuro se propone analizar la resistencia al desgaste de los recubrimientos, su durabilidad y ángulo de deslizamiento, mejorando sus propiedades hidrofóbicas.

Palabras clave: Recubrimientos ultra-hidrofóbicos; Diseño de experimentos; Nanopartículas de SiO_2 ; Método sol-gel; Transparencia



1. Introduction

Material surfaces are highly exposed to environmental conditions [1], contamination, dirt [2-3], dust [4], sand [5], acidic water, oily substances [6], etc. In general, many of these conditions are undesirable since they negatively influence the useful life of the material and its performance [7-8]. Some surfaces are more often faced with certain substances and are therefore more prone to damage [7]. That is why, for some years now, scientists have tried to create surfaces that meet certain needs [8], starting from knowing the characteristics and abilities of some plants and animals.

One of the most studied conditions in recent times is high-hydrophobic condition. Ultra-hydrophobic (UH) surfaces show values of SCA between 120-150° [9], while in superhydrophobic (SH) surfaces are above of 150° [2][6][12-19] between the solid phase and the liquid phase. This characteristic allows a wide number of applications, including self-cleaning [8][10-16], drag reduction [8][12][17], anti-corrosion [8][10][18-21], transparency [8][22-23], anti-icing [16][18-20], oil-water separation [17-18] and so on. This type of surface influences the reduction of maintenance costs [24] and increases the useful life of the materials [25].

There are two approaches to achieve high-hydrophobic conditions: (i) increase surface roughness [26-29], (ii) decrease surface tension [20][30-33]. The first approach is related to the idea of reducing, as much as possible, the contact area between liquid and solid, and in turn, being able to create spaces in which air bubbles can be located [20] [31][34-36] that serve as a barrier (protects the drop from morphological irregularities that can undo them). The second approach is closer to the chemical composition,

which determines the adhesion forces present in the contact area [37-40].

There are compounds that make it possible to achieve superhydrophobic characteristics through the application of the aforementioned approaches, specifically the use of silanes. Vouvoudi et al. [1] manufactured a superhydrophobic coating for the protection of the stone-built cultural heritage. They reported SCA of 170° approximately. To do this, they mixed tetraethyl orthosilicate (TEOS) and 1H, 1H, 2H, 2H-perfluorooctyl tri-ethoxy silane (FAS). Finally, the versatility of the solution allowed excellent results on at least 3 more substrates [1]. Zhu et al. [26] created a transparent SH coating with good mechanical properties. The silane used was polydimethylsiloxane (PDMS), which is not contaminating like those containing fluorine. The modification achieved by this compound allowed reaching values of SCA higher than 160° and transparency levels higher than 76% [26].

In this article, we report the development of UH and transparent coatings through SCA optimization based on a general full factorial design. The coatings show SCA values greater than 140° and transparency values greater than 65%. The corresponding characterizations were carried out.

2. Methodology

The Figure 1 illustrates the steps to follow in the present investigation.

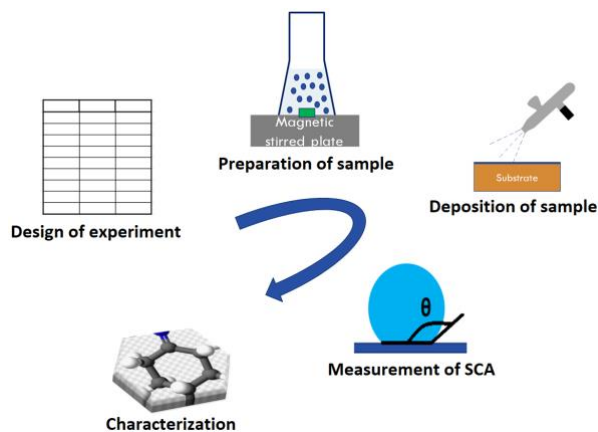


Figure 1. Methodology

2.1 Materials

The following materials were used for the preparation of the coatings: tetraethyl orthosilicate (TEOS), (98% from Sigma-Aldrich) as a precursor for SiO₂ nanoparticles; Ammonium hydroxide (NH₄OH), (NH₃ content 28-30% from Sigma Aldrich®) that influences the size of the nanoparticles; 1H, 1H, 2H, 2H-perfluorodecyltriethoxysilane (AC-FAS) (97% from Matrix Scientific®) is applied as a surface modifier; isopropyl alcohol (IPA) and deionized water (DIW).

2.2 Equipments

Stirring hot plate (model PC-420D, CORNING®). Ultrasonic cleaning bath (model TS-2.5L), truSonik®.

2.3 Design of experiment (DOE)

The DOE chosen was a general full factorial design. The Figure 2 illustrates a general analysis for our investigation.

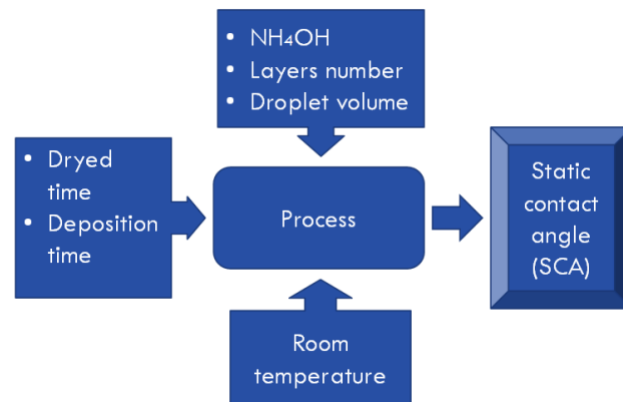


Figure 2. General model of the investigation process

The inputs for this design were the drying time of coatings and deposition time between layers. The controllable factors were the NH₄OH concentration, the number of layers and the applied droplet volume to measure the static contact angle. As an uncontrollable factor, it was only defined at room temperature. The output variable was established as the SCA. All prepared samples were made up to a volume of 50 ml. Table 1 shows the agent volumes in each sample.

Table 1. Agent volumes

Samples	IPA (ml)	DIW (ml)	TEOS (ml)	AC FAS (ml)	NH ₄ OH (ml)
M1	36.8	11.71	1	0.15	0.5
M2	37.04	11.71	1	0.15	0.25
M3	37.24	11.71	1	0.15	0.05
M4	37.265	11.71	1	0.15	0.025

The only difference between samples is the NH₄OH content. This difference made it possible to assess the influence of NH₄OH on SCA.

2.4 Preparation of samples

The preparation procedure proposed by Ge et al. [41]. Prior to the preparation, a deep wash of all the necessary elements (glass Erlenmeyer



flasks, pipette tips, magnetic stirrers) was carried out to develop the preparation of the samples. The washing was carried out with DIW andalconox® detergent, and subsequently they were rinsed with DIW and IPA. The preparation of the solutions was started by stirring a mixture of IPA and DIW at 500 rpm, in a 100 ml glass Erlenmeyer flask, for 10 min. Then NH₄OH and TEOS were added in the order mentioned and kept at the same angular stirring speed for 24 h. After the planned time, the AC-FAS was added and 48 h were waited to turn off the stirring hot plate machine, in this way the preparation process was concluded. The entire process was carried out at room temperature.

2.5 Spray Deposition

Prior depositing the solution on the substrate (26 x 76 x ± 1-1.2 mm glass slides, from Lauka®), it was placed in the ultrasonic cleaning bath machine in order to achieve a greater degree of homogeneity of the solution. The spray gun was also washed as an essential element of the selected method. The spray method was carried out at 15 cm from the substrate placed horizontally, the firing pressure was 0.2 MPa at room temperature. The deposition time between coats was set at 10 min, while the final drying time (time in which the SCAs were measured was 24 h). The drying was carried out naturally (air).

2.6 Characterization

The chemical composition and morphology of the surface, and NPs size analysis were carried out with the use of the field emission scanning electron microscope (FESEM) (JEOL® brand, model JSM-7000F) and energy dispersive spectrometer (EDS). The volume ratio between IPA and samples was 10: 1, and it was deposited on a carbon adhesive tape. Fourier transform infrared (FT-IR) spectrophotometer (BUCK Scientific®, model 530), it was used to identify the functional groups in a wavenumber interval of 600-4000 cm⁻¹, and a

resolution of 0.8 cm⁻¹; the samples had to be prepared with potassium bromide (KBr). Ultraviolet visible light (UV-vis) spectrophotometer (series AF1311015) was used to determine the light transmittance in a range of 380-760 nm with intervals of 1 nm. SCA measurement was achieved with a Profile Projector (Mitutoyo Corporation®, model PH-A14).

3 Results and Discussion

3.1 Statistical analysis

Images for SCA measurement were obtained using a profile projector and analyzed with the ImageJ software. Table 2 shows the SCA values.

Table 2. Static contact angles

Samples	SCA-5 µl (°)	SCA-10 µl (°)
M1 (2 layers)	147±2	146.2±3
M1 (4 layers)	152.55±1	150.6±2
M2 (2 layers)	148.4±2	148.2±2
M2 (4 layers)	150±2	150.3±2
M3 (2 layers)	146.8±3	143.3±2
M3 (4 layers)	151.4±2	151±1
M4 (2 layers)	145.9±3	144.1±3
M4 (4 layers)	151.8±1	151.7±1

Table 2 presents all the values in a range of 141-153° when the highest value was 152.55 ± 1° and it was reached in M1. Table 2 shows that, as the number of layers increases, the SCA increases. The number of layers is a factor that can be directly related to the thickness of the coating, because, as the number of layers increases, the thickness increases. Ge et al. [41] investigated the influence of thickness on SCA for a coating obtained from the mixture of two



silanes, TEOS and (heptadecafluoro-1,1,2,2-tetrahydrodecyl)triethoxysilane (HDFTES), with a stringed SiO₂ NPs. The result shows that when increasing the thickness of 2-8 μm, the SCA increased from 160.5-165.5° approximately [41]. This result coincides with the result obtained in this investigation. Purcar et al. [42] reported the influence of thickness on the SCA of SiO₂-based coatings obtained from TEOS and modified with alkoxysilane mixtures using the sol-gel method. The alkoxysilanes used were methyl triethoxysilane (MTES), octyltriethoxysilane (OTES), vinyltrimethoxysilane (VTMES), and hexadecyltrimethoxysilane (HDTMES). The thicknesses for TEOS/MTES/OTES, TEOS/MTES/VTMES and TEOS/MTES/HDTMES were 3522.8, 1288.0 and 1584.9 nm respectively; their respective SCAs for the thicknesses obtained were 104, 88 and 106° [42]. The presence of a second factor included in the analysis caused a change in the results. This time the study included, in addition to thickness, the type of alkoxysilane, which led to the loss of the relationship obtained in the present study and increases in SCA were not achieved with increasing thickness.

Using the Minitab® 17 software, it performed the general full factorial design to determine if the factors taken into account significantly influence the response variable. The experiment was randomized and replicated to ensure a more reliable test. Figure 3 presents the results of the analysis.

Source	DF	Adj SS	Adj MS	P-Value
Model	15	232.520	15.501	0.000
Linear	5	187.300	37.460	0.000
NH4OH	3	9.488	3.163	0.002
Capa	1	166.531	166.531	0.000
Gota	1	11.281	11.281	0.000
2-Way Interactions	7	32.812	4.687	0.000
NH4OH*Capa	3	22.711	7.570	0.000
NH4OH*Gota	3	7.221	2.407	0.006
Capa*Gota	1	2.880	2.880	0.016
3-Way Interactions	3	12.408	4.136	0.000
NH4OH*Capa*Gota	3	12.408	4.136	0.000
Error	16	6.380	0.399	
Total	31	238.900		

Figure 3. P-Value analysis

Taking into account a confidence level of 95%, the significant factors will be those that do not exceed the level of significance (0.05). As can be seen, the three factors proposed in the experiment showed p-values lower than the reference value mentioned above. Similarly, double and triple interactions have p-values lower than the reference value. All this information allows us to declare that all the factors and their interactions will be significant for the response variable. It also generated the main effects plot for SCA to more easily observe the influence of each factor on the response variable. Figure 4 presents the directions we can choose from each factor to increase SCA.

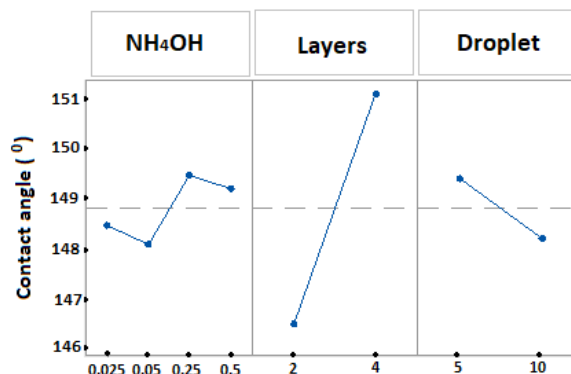


Figure 4. Main effects plot for SCA (fitted means)

Figure 4 presents the behavior of each factor in this investigation. The NH₄OH factor showed better SCA values at the levels with the highest concentration of NH₃; the number of layers confirmed that as it increased, the values of the response variable increased too; while an increase in drop volume tends to decrease SCA. These SCA results make it possible to ensure that the three factors influence the achievement of ultrahydrophobicity (120 < SCA ≤ 150°); in addition, in the particular case of number of layers, 4 layers allowed achieving superhydrophobicity (SCA > 150°). Figure 5 allows a double interaction analysis of the factors.

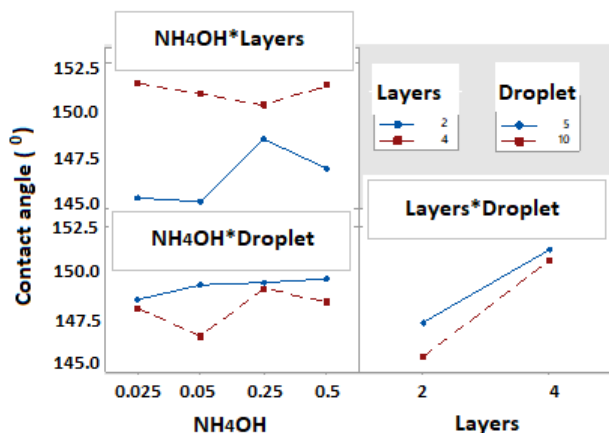


Figure 5. Interaction plot for SCA (fitted means)

This figure shows the interactions between factors, and it is evidenced that the least interaction is established between NH_4OH and number of layers. On the other hand, between number of layers and drop volume a certain closeness and similar direction is perceived, which allows to ensure that it is the interaction that has the most effect on SCA; the highest SCA values were reached for this interaction.

The response variable was maximized to determine the 5 best combinations of factors. Figure 6 shows the response optimizer.

Solution	NH_4OH	Layers	Droplet	SCA fit
1	0.5	4	5	152.55
2	0.025	4	10	151.80
3	0.025	4	5	151.35
4	0.05	4	5	151.15
5	0.05	4	10	150.85

Figure 6. Response optimizer.

Fig. 6 allows determining the combinations of factors with the highest SCA values. The response optimizer presented the 5 highest SCA values in the study. All combinations met the maximum number of layers deposited (4 layers), this confirms the idea that to achieve superhydrophobic surfaces it was necessary to

apply 4 layers of coatings. The highest value obtained was $152,55^\circ$.

3.2 Functional groups analysis

The analysis of the functional groups was carried out with a FT-IR. In Figure 7 the spectrum generated by the SiO_2 NPs is observed.

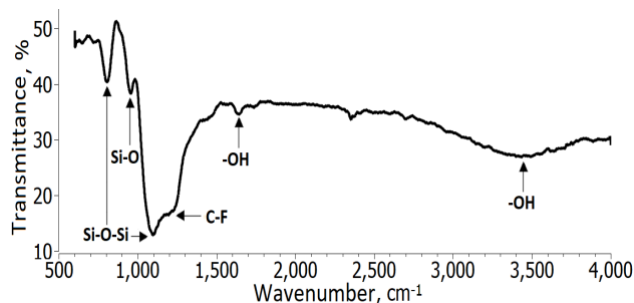


Figure 7. FT-IR spectrum (sample M3)

In the FT-IR spectrum of glass substrate, a broad band were identified from $2750\text{-}3800\text{ cm}^{-1}$ with center at approximately 3400 cm^{-1} , corresponding to the hydroxyl stretching ($-\text{OH}$ stretching vibrations) [1][37-39], then another $-\text{OH}$ group was observed around 1630 cm^{-1} . The C-F stretching vibrations peak at 1204 cm^{-1} was easily recognized in the spectrum [41][43]; these groups are characterized by having low energy, they are attributed a decrease in the surface energy of the coating. The peak at 1100 cm^{-1} was attributed to the most characteristic peak of the SiO_2 nanoparticles [1][37-38], which is assigned to the asymmetric stretching, symmetric stretching and bending vibration. Finally, two more peaks were located below 1000 cm^{-1} : (i) at 950 cm^{-1} (Si-O bond) [42] and (ii) at 793 cm^{-1} belong to vibrations Si-O-Si bonds [1][26][41][44] attributed to the bending vibrations.



3.3 Chemical composition

The chemical composition was evaluated with the use of FESEM-EDS. The solution was analyzed before adding the AC-FAS and another with all the reagents that make up the coating. In addition, images of the distribution of each chemical element in each sample were obtained, as shown in Figure 8.

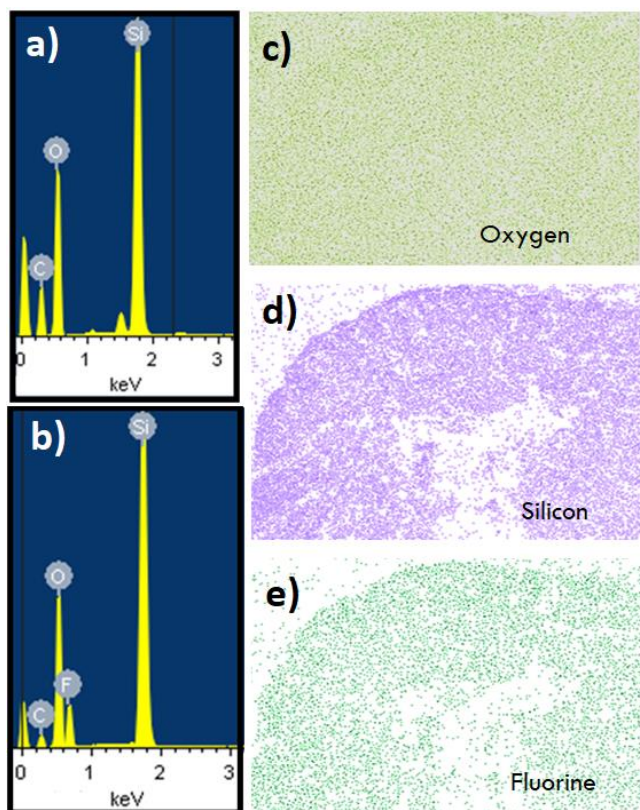


Figure 8. FESEM (EDS mapping) images (sample M3): (a) Solución sin AC-FAS, (b) solución con AC-FAS, (c) Oxygen map, (d) Silicon map, and (e) Fluorine map.

In Figure 10 (a, b), the presence of Si, O and C is observed, while F only appears in Figure 10b due to the addition of AC-FAS. All chemicals were evenly distributed over the entire surface, suggesting that the preparation method used was appropriate to achieve a uniform coating.

3.4 Surface morphological study

The morphological analysis was carried out in FESEM. Figure 9 showed the surface morphology of the sample M3.

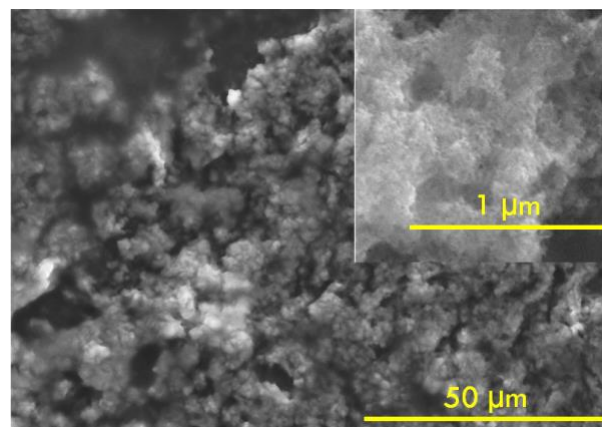


Figure 9. FESEM (secondary electrons) images (sample M3)

The images obtained in SEM showed a large agglomeration of particles. This agglomeration can be a consequence of the addition of AC-FAS. This agglomeration can also decrease the degree of hydrophobicity, and can be the cause of a decrease in the percentage of light transmittance. Finally, particle agglomeration made particle size determination impossible.

3.5 Transparency analysis

The transparency of all samples (2 and 4 layers) was determined by using the UV-vis spectrophotometer; all analysis was performed in the wavelength interval 380-760 nm. Figure 10 shows the transmittance spectra of the coatings.

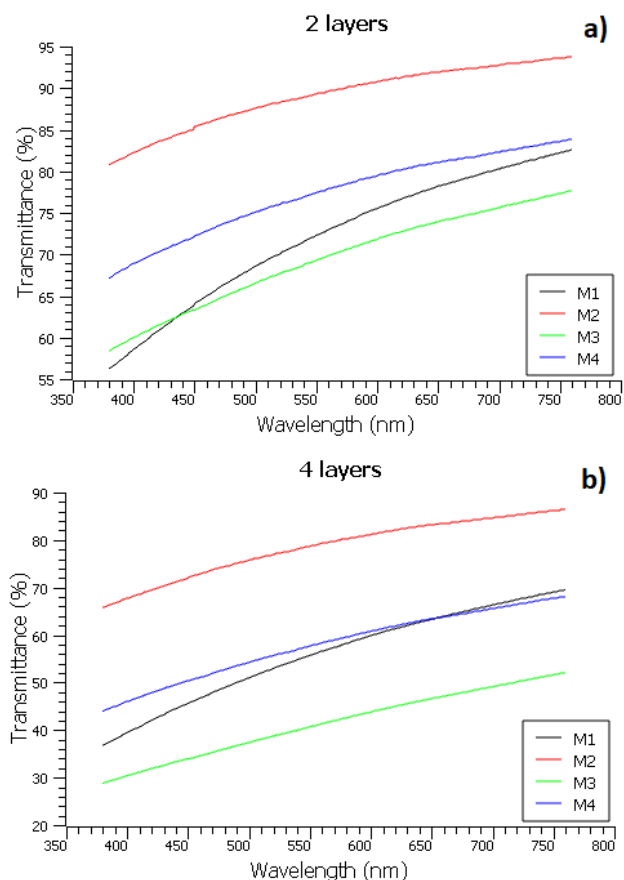


Figure 10. Transmittance spectra UV-vis: (a) 2 layers, (b) 4 layers.

As shown in Figure 10a, the M2 lost 11% of the transmittance compared to an uncoated glass (100%), for 89% of transmittance, approximately. The other samples presented average values in a range of 68-80%. When the number of layers was increased to 4 (Figure 10b), there was a loss of transmittance of 23% (sample 2), while the others were less than 60%. These results suggested that by increasing the number of layers there was an increase in surface roughness, which led to an increased light scattering, thus decreasing the light transmittance. In this case, the number of layers is analogous to the number of cycles, which increases the thickness of the coating as it increases. H. Teisala et al. [45] transparency was investigated using UV-vis spectrophotometer for different Si/Ti ratios. The results were obtained by

applying 1 and 5 coating cycles on the substrate. For 1 cycle, all transmittance values were greater than 98% for wavelengths greater than 500 nm. For 5 cycles, 97% were obtained in Si-100% and 79% with Si-1%, which indicated a decrease in transmittance as the concentration of Si in the coatings decreased [45]. It can be noted that this result agrees with the result obtained in our study, the increase in the number of cycles has a negative effect on the level of transparency [45]. Ge et al. [41] investigated the influence of thickness on the transparency results of coatings made with a TEOS/HDFTES solution with stringed SiO₂ nanoparticles. The range in which the measurements were made was 3-8 μm and it was observed that as the thickness increased there was a decrease in transmittance; the transmittance obtained was approximately 91.5% at 550 nm for a thickness of 5 μm [41]. This result also confirms our result.

4 Conclusions

Ultra-hydrophobic coatings based on SiO₂ nanoparticles were developed using the sol-gel method. The SCA obtained exceeded 140⁰, reaching values above 150⁰ (super-hydrophobicity). The influence of three factors (NH₄OH, number of layers and droplet volume) on the ACS was analyzed using a general full factorial design with a 95% confidence level. All the factors were statistically significant for the output variable. By increasing NH₄OH there was an increase in SCA; when the number of layers increased, the SCA also increased; while with increasing droplet volume, SCA decreased. Other studies show similar results for the number of layers because it is related to the increase in surface roughness; This factor is also the main responsible for achieving SCA values higher than 150⁰.



The FESEM images showed an excessive agglomeration of particles, an aspect that must have had a negative impact on the results of contact angles and that prevented the determination of the particle size; agglomeration was attributed to AC-FAS.

The analysis of functional groups permitted to identify SiO₂ nanoparticles, which shows that the sol-gel method is appropriate for this objective; It was possible to verify the presence of C-F groups, to which the decrease in the surface energy of the coating and the high degree of hydrophobicity due to its low energy are attributed.

Transparency levels of 68-89% were achieved. The number of layers negatively influenced the level of transparency, reducing the transmittance of sample M2 from 89 to 77 for 2 and 4 layers respectively. This result was consistent with studies conducted by other researchers.

In this study, we managed to include a factor not widely studied: droplet volume. In addition, the coatings developed can be implemented in applications such as self-cleaning, anti-reflection, anti-corrosion, among others.

5. Acknowledgements

To Universidad Autónoma de Ciudad Juárez/Instituto de Ingeniería y Tecnología, and CONACyT.

6. Authorship and Contribution

Jose Felix Magdaleon Loreda: Conceptualization, methodology, validation, formal analysis, research, original draft, revision-edition, visualization, project supervision-administration, data analysis. *Delfino Cornejo Monroy:* Conceptualization, methodology, research, revision-edition, project supervision-administration.

References

- [1] E. C. Vouvoudi, F. G. Adamopoulos, E. Pavlidou, D. S. Achilias, and I. Karapanagiotis, "TEOS-Based Superhydrophobic Coating for the Protection of Stone-Built Cultural Heritage," *Coatings*, pp. 1-12, 2021. <https://doi.org/10.3390/coatings11020135>
- [2] I. S. Bayer, "Superhydrophobic Coatings from Ecofriendly Materials and Processes: A Review," *Adv. Mater. Interfaces*, vol. 7, no. 13, pp. 1-25, 2020. <https://doi.org/10.1002/admi.202000095>
- [3] B. Li and J. Zhang, "Durable and self-healing superamphiphobic coatings repellent even to hot liquids," *Chem. Commun.*, vol. 52, no. 13, pp. 2744-2747, 2016. <https://doi.org/10.1039/C5CC09951J>
- [4] M. R. Ghadimi and A. Dolati, "Preparation and characterization of superhydrophobic and highly oleophobic FEVE-SiO₂ nanocomposite coatings," *Prog. Org. Coatings*, vol. 138, no. April 2019, p. 105388, 2020. <https://doi.org/10.1016/j.porgcoat.2019.105388>
- [5] M. Ferrari and F. Cirisano, "High transmittance and highly amphiphobic coatings for environmental protection of solar panels," *Adv. Colloid Interface Sci.*, vol. 286, p. 102309, 2020. <https://doi.org/10.1016/j.cis.2020.102309>
- [6] T. N. H. Lo, H. S. Hwang, J. Lee, and I. Park, "Synthesis of new semi-fluorinated polysilazanes and their amphiphobic coating applications," *Prog. Org. Coatings*, vol. 148, no. June, p. 105853, 2020. <https://doi.org/10.1016/j.porgcoat.2020.105853>
- [7] X. Han, J. Peng, S. Jiang, J. Xiong, Y. Song, and X. Gong, "Robust Superamphiphobic Coatings Based on Raspberry-like Hollow SnO₂Composites," *Langmuir*, vol. 36, no. 37, pp. 11044-11053, 2020. <https://doi.org/10.1021/acs.langmuir.0c01923>
- [8] Y. Bai, H. Zhang, Y. Shao, H. Zhang, and J. Zhu, "Recent progresses of superhydrophobic coatings in different application fields: An overview," *Coatings*, vol. 11, no. 2, pp. 1-30, 2021. <https://doi.org/10.3390/coatings11020116>



[9] L. Álvarez-Gil, J. Ramírez, and P. Fernández-Morales, "Ultra-hydrophobic aluminum foam development for potential application in continuous water-oil separation processes," *Surfaces and Interfaces*, vol. 26, no. July, 2021. <https://doi.org/10.1016/j.surfin.2021.101362>

[10] V. Sharma et al., "Recent progress in nano-oxides and CNTs based corrosion resistant superhydrophobic coatings: A critical review," *Prog. Org. Coatings*, vol. 140, no. December 2019, p. 105512, 2020. <https://doi.org/10.1016/j.porgcoat.2019.105512>

[11] J. Zhang, B. Yu, Z. Gao, B. Li, and X. Zhao, "Durable, transparent, and hot liquid repelling superamphiphobic coatings from polysiloxane-modified multiwalled carbon nanotubes," *Langmuir*, vol. 33, no. 2, pp. 510-518, 2017. <https://doi.org/10.1021/acs.langmuir.6b04213>

[12] Y. Wang and X. Gong, "Special oleophobic and hydrophilic surfaces: approaches, mechanisms, and applications," *J. Mater. Chem. A*, vol. 5, no. 8, pp. 3759-3773, 2017. <https://doi.org/10.1039/C6TA10474F>

[13] W. Yao, L. Li, O. L. Li, Y. W. Cho, M. Y. Jeong, and Y. R. Cho, "Robust, self-cleaning, amphiphobic coating with flower-like nanostructure on micro-patterned polymer substrate," *Chem. Eng. J.*, vol. 352, no. June, pp. 173-181, 2018. <https://doi.org/10.1016/j.cej.2018.07.001>

[14] F. Cirisano, A. Benedetti, L. Liggieri, F. Ravera, E. Santini, and M. Ferrari, "Amphiphobic coatings for antifouling in marine environment," *Colloids Surfaces A Physicochem. Eng. Asp.*, vol. 505, pp. 158-164, 2016. <https://doi.org/10.1016/j.colsurfa.2016.03.045>

[15] J. Li et al., "Superhydrophobic Methylated Silica Sol for Effective," 2020. <https://doi.org/10.3390/ma13040842>

[16] P. Nguyen-Tri et al., "Recent progress in the preparation, properties and applications of superhydrophobic nano-based coatings and surfaces: A review," *Prog. Org. Coatings*, vol. 132, no. January, pp.

235-256, 2019. <https://doi.org/10.1016/j.porgcoat.2019.03.042>

[17] E. Vazirinasab, R. Jafari, and G. Momen, "Application of superhydrophobic coatings as a corrosion barrier: A review," *Surf. Coatings Technol.*, vol. 341, no. October 2017, pp. 40-56, 2018. <https://doi.org/10.1016/j.surfcoat.2017.11.053>

[18] G. Barati Darband, M. Aliofkhaezraei, S. Khorsand, S. Sokhanvar, and A. Kaboli, "Science and Engineering of Superhydrophobic Surfaces: Review of Corrosion Resistance, Chemical and Mechanical Stability," *Arab. J. Chem.*, vol. 13, no. 1, pp. 1763-1802, 2020. <https://doi.org/10.1016/j.arabj.2018.01.013>

[19] S. Das, S. Kumar, S. K. Samal, S. Mohanty, and S. K. Nayak, "A Review on Superhydrophobic Polymer Nanocoatings: Recent Development and Applications," *Ind. Eng. Chem. Res.*, vol. 57, no. 8, pp. 2727-2745, 2018. <https://doi.org/10.1021/acs.iecr.7b04887>

[20] A. Hooda, M. S. Goyat, J. K. Pandey, A. Kumar, and R. Gupta, "A review on fundamentals, constraints and fabrication techniques of superhydrophobic coatings," *Prog. Org. Coatings*, vol. 142, no. January, p. 105557, 2020. <https://doi.org/10.1016/j.porgcoat.2020.105557>

[21] S. P. Dalawai et al., "Recent Advances in durability of superhydrophobic self-cleaning technology: A critical review," *Prog. Org. Coatings*, vol. 138, no. May 2019, p. 105381, 2020. <https://doi.org/10.1016/j.porgcoat.2019.105381>

[22] Z. Liang, M. Geng, B. Dong, L. Zhao, and S. Wang, "Transparent and robust SiO₂/PDMS composite coatings with self-cleaning," *Surf. Eng.*, vol. 36, no. 6, pp. 643-650, 2020. <https://doi.org/10.1080/02670844.2019.1691367>

[23] U. Mehmood, F. A. Al-Sulaiman, B. S. Yilbas, B. Salhi, S. H. A. Ahmed, and M. K. Hossain, "Superhydrophobic surfaces with antireflection properties for solar applications: A critical review," *Sol. Energy Mater. Sol. Cells*, vol. 157, pp. 604-623, 2016. <https://doi.org/10.1016/j.solmat.2016.07.038>



[24] X. Zhao, D. S. Park, J. Choi, S. Park, S. A. Soper, and M. C. Murphy, "Robust, transparent, superhydrophobic coatings using novel hydrophobic/hydrophilic dual-sized silica particles," *J. Colloid Interface Sci.*, vol. 574, pp. 347-354, 2020. <https://doi.org/10.1016/j.jcis.2020.04.065>

[25] W. Lin, X. Zhang, Q. Cai, W. Yang, and H. Chen, "Dehydrogenation-driven assembly of transparent and durable superhydrophobic ORMOSIL coatings on cellulose-based substrates," *Cellulose*, vol. 27, no. 13, pp. 7805-7821, 2020. <https://doi.org/10.1007/s10570-020-03288-2>

[26] T. Zhu et al., "A transparent superhydrophobic coating with mechanochemical robustness for anti-icing, photocatalysis and self-cleaning," *Chem. Eng. J.*, vol. 399, no. June, p. 125746, 2020. <https://doi.org/10.1016/j.cej.2020.125746>

[27] J. Liu, X. Jiao, F. Cheng, Y. Fan, Y. Wu, and X. Yang, "Fabrication and performance of UV cured transparent silicone modified polyurethane-acrylate coatings with high hardness, good thermal stability and adhesion," *Prog. Org. Coatings*, vol. 144, no. March, p. 105673, 2020. <https://doi.org/10.1016/j.porgcoat.2020.105673>

[28] G. Fortunato, V. Marroccoli, F. Corsini, S. Turri, and G. Griffini, "A facile approach to durable, transparent and self-healing coatings with enhanced hardness based on Diels-Alder polymer networks," *Prog. Org. Coatings*, vol. 147, no. June, 2020. <https://doi.org/10.1016/j.porgcoat.2020.105840>

[29] J. Dong et al., "Colorful superamphiphobic coatings with low sliding angles and high durability based on natural nanorods," *ACS Appl. Mater. Interfaces*, vol. 9, no. 2, pp. 1941-1952, 2017. <https://doi.org/10.1021/acsami.6b13539>

[30] N. Pratiwi, Zulhadjri, S. Arief, Admi, and D. V. Wellia, "Self-cleaning material based on superhydrophobic coatings through an environmentally friendly sol-gel method," *J. Sol-Gel Sci. Technol.*, vol. 96, no. 3, pp. 669-678, 2020. <https://doi.org/10.1007/s10971-020-05389-7>

[31] F. Sharifianjazi et al., "Effects of Sr and Mg dopants on biological and mechanical properties of SiO₂-CaO-P₂O₅ bioactive glass," *Ceram. Int.*, vol. 46, no. 14, pp. 22674-22682, 2020. <https://doi.org/10.1016/j.ceramint.2020.06.030>

[32] A. Jaafar, C. Hecker, P. Árki, and Y. Joseph, "Sol-gel derived hydroxyapatite coatings for titanium implants: A review," *Bioengineering*, vol. 7, no. 4, pp. 1-23, 2020. <https://doi.org/10.3390/bioengineering7040127>

[33] C. Chen et al., "Microstructure-controllable nanocomplexes bulk possessed with durable superhydrophobicity," *Chem. Eng. J.*, vol. 389, no. January, p. 124420, 2020. <https://doi.org/10.1016/j.cej.2020.124420>

[34] L. Vivar Mora et al., "Impact of silica nanoparticles on the morphology and mechanical properties of sol-gel derived coatings," *Surf. Coatings Technol.*, vol. 342, no. 2017, pp. 48-56, 2018. <https://doi.org/10.1016/j.surfcoat.2018.02.080>

[35] F. Wang et al., "A superhydrophobic coating to create multi-functional materials with mechanical/chemical/physical robustness," *Chem. Eng. J.*, vol. 381, no. March 2019, p. 122539, 2020. <https://doi.org/10.1016/j.cej.2019.122539>

[36] J. Zhang et al., "Preparation of humidity, abrasion, and dust resistant antireflection coatings for photovoltaic modules via dual precursor modification and hybridization of hollow silica nanospheres," *Sol. Energy Mater. Sol. Cells*, vol. 192, no. June 2018, pp. 188-196, 2019. <https://doi.org/10.1016/j.solmat.2018.12.032>

[37] Y. Zhang, B. Dong, S. Wang, L. Zhao, L. Wan, and E. Wang, "Mechanically robust, thermally stable, highly transparent superhydrophobic coating with low-temperature sol-gel process," *RSC Adv.*, vol. 7, no. 75, pp. 47357-47365, 2017. <https://doi.org/10.1039/C7RA08578H>

[38] D. Adak, R. Bhattacharyya, H. Saha, and P. S. Maiti, "Sol-gel processed silica based highly transparent self-cleaning coatings for solar glass covers," *Mater. Today Proc.*, vol. 33, pp. 2429-2433,



2019.

<https://doi.org/10.1016/j.matpr.2020.01.331>

[39] S. Arya et al., "Review-Influence of Processing Parameters to Control Morphology and Optical Properties of Sol-Gel Synthesized ZnO Nanoparticles," ECS J. Solid State Sci. Technol., vol. 10, no. 2, p. 023002, 2021.

<https://doi.org/10.1149/2162-8777/abe095>

[40] M. Chodkowski, K. Terpiłowski, and S. Pasieczna-Patkowska, "Fabrication of transparent polysiloxane coatings on a glass support via the sol-gel dip coating technique and the effect of their hydrophobization with hexamethyldisilazane," Physicochem. Probl. Miner. Process., vol. 56, no. 6, pp. 76-88, 2020.

<https://doi.org/10.37190/ppmp/126806>

[41] D. Ge, L. Yang, Y. Zhang, Y. Rahmawan, and S. Yang, "Transparent and superamphiphobic surfaces from one-step spray coating of stringed silica nanoparticle/sol solutions," Part. Part. Syst. Charact., vol. 31, no. 7, pp. 763-770, 2014.

<https://doi.org/10.1002/ppsc.201300382>

[42] R. Manea et al., "Preparation and Characterization of Some Sol-Gel Modified Silica Coatings Deposited on Polyvinyl Chloride (PVC) Substrates," Coatings, 2021.

<https://doi.org/10.3390/coatings11010011>

[43] A. K. Schmidt-Verma et al., "High-Temperature Ultrahydrophobic Ceramic Coatings from Surface-Functionalized MgAl₂O₄ Nanoparticles," Adv. Eng. Mater., vol. 23, no. 2, pp. 2-9, 2021.

<https://doi.org/10.1002/adem.202000738>

[44] L. Ye, Y. Zhang, C. Song, Y. Li, and B. Jiang, "A simple sol-gel method to prepare superhydrophilic silica coatings," Mater. Lett., vol. 188, pp. 316-318, 2017.

<https://doi.org/10.1016/j.matlet.2016.09.043>

[45] H. Teisala et al., "Ultrafast Processing of Hierarchical Nanotexture for a Transparent Superamphiphobic Coating with Extremely Low Roll-Off Angle and High Impalement Pressure," Adv. Mater., vol. 30, no. 14, pp. 1-8, 2018.

<https://doi.org/10.1002/adma.201706529>

Derechos de Autor (c) 2022 José Felix Magdaleon Loredó, Delfino Cornejo Monroy



Este texto está protegido por una licencia [Creative Commons 4.0](https://creativecommons.org/licenses/by/4.0/)

Usted es libre para Compartir —copiar y redistribuir el material en cualquier medio o formato— y Adaptar el documento —remezclar, transformar y crear a partir del material— para cualquier propósito, incluso para fines comerciales, siempre que cumpla la condición de:

Atribución: Usted debe dar crédito a la obra original de manera adecuada, proporcionar un enlace a la licencia, e indicar si se han realizado cambios. Puede hacerlo en cualquier forma razonable, pero no de forma tal que sugiera que tiene el apoyo del licenciante o lo recibe por el uso que hace de la obra.

[Resumen de licencia - Texto completo de la licencia](#)